This is the accepted version of the following article:

Belleri A, Cornali F, Passoni C, Marini A, Riva P. Evaluation of out-of-plane seismic performance of column-to-column precast concrete cladding panels in one-storey industrial buildings. Earthquake Engng Struct Dyn. 2017;1–21. DOI: 10.1002/eqe.2956

which has been published in final form at https://doi.org/10.1002/eqe.2956. This article may be used for non-commercial purposes in accordance with the Wiley Self-Archiving Policy

Evaluation of out-of-plane seismic performance of column-to-column precast concrete cladding panels in one-storey industrial buildings

Andrea Belleri (*), Fabrizio Cornali, Chiara Passoni, Alessandra Marini, Paolo Riva

Department of Engineering and Applied Sciences, University of Bergamo,
Viale Marconi 5, 24044, Dalmine – Italy

Abstract

Recent earthquakes in Italy (L'Aquila 2009 and Emilia 2012) highlighted the vulnerability of precast cladding panels, typically associated with a connection system not designed to account for displacement and rotation compatibility between the panels and the supporting structure. Experimental investigations were carried out in the past to investigate the in-plane performance of cladding panels and design recommendations have been made accordingly; however, in the case of out-of-plane seismic loads, the load demand is commonly evaluated in the design practice by means of formulations for non-structural components.

This paper summarises the results obtained from parametric analyses conducted to estimate the out-of-plane load demand in column-to-column cladding panels typical of one-storey commercial and industrial buildings. Empirical equations suitable for both new and existing panels are proposed and compared with the design equations given in Eurocode 8 and ASCE 7. The paper also considers the effects of the development of plastic hinges at the column base and of the roof flexibility on the load demand in panel-to-column connections. The roof flexibility may generate the torsion of the panels, consequently an analytical procedure to account for such effects is proposed. Finally, general design recommendations are made.

Keywords: Precast concrete structures; Cladding connections; Cladding panels; Out-of-plane loads; Roof flexibility; Seismic vulnerability.

1. Introduction

Recent earthquakes in Italy (L'Aquila 2009 and Emilia 2012) highlighted the vulnerability of precast reinforced concrete (RC) structures which are not designed according to the modern seismic codes as reported in numerous studies (Toniolo and Colombo 2012; Marzo et al. 2012; Savoia et al. 2012; Liberatore et al. 2013; Magliulo et al. 2014a; Belleri et al. 2014a; Bournas et al. 2014; Casotto et al. 2015; Minghini et al. 2016; Nastri et al. 2017; Palanci et al. 2017). The main vulnerabilities, which caused both local and global collapses, are related to the lack of effective horizontal load transfer mechanism between precast elements and to the lack of displacement and rotation compatibility among structural elements and between structural and non-structural elements (Belleri et al. 2014b, 2015; Brunesi et al. 2015; Colombo et al. 2016).

The structural layout of the precast concrete structures considered herein (Bellotti et al. 2009; Negro et al. 2013; Belleri 2017), typical of industrial and commercial buildings, is composed of cantilever columns pin-connected (Psycharis and Mouzakis 2012; Magliulo et al. 2014b; Zoubek et al. 2015) to prestressed RC beams spanning in one direction, which support prestressed concrete roof elements spanning in the transverse direction. The columns are embedded in a grouted socket left in the footing (Osanai et al. 1996) or connected to the foundation by means of mechanical devices or grouted sleeves (Metelli et al. 2011; Belleri and Riva 2012; Dal Lago et al. 2016). Industrial and commercial precast concrete buildings are typically characterized by higher inter-storey height and higher roof flexibility compared to RC buildings. This leads to a generally high lateral flexibility, which makes displacement compatibility between connected elements an important aspect to be analysed.

The cladding system is typically made up of precast RC panels, two types of panels are considered: panels spanning laterally, connecting adjacent columns, and panels spanning vertically, connecting the grade beam to the roof beam; in the European practice, the latter is referred to as "vertical panel" while the former as "horizontal panel", respectively (Colombo et al. 2016). Precast cladding panels are mainly reinforced with steel welded-wire-mesh (Riva et al. 2001), installed on the outside of the building and connected to the main structural elements. The in-plane interaction between cladding and structural systems is categorized as (Arnold 1989): *completely separated cladding*, *accidentally participating cladding* (Belleri et al. 2016)*, controlled participating cladding* (Ferrara et al. 2011; Scotta et al. 2015) and *fully participating cladding* (Biondini et al. 2013; Magliulo et al. 2015). In regions of high seismicity (NIST GCR 95-681), connections enabling relative movements between the elements are commonly adopted, i.e. *completely separated cladding* according to Arnold (1989).

In past European construction practices, the cladding system was primarily designed for vertical gravity loads and to avoid panel overturning due to out-of-plane wind loads or, more recently, seismic loads. Displacement compatibility associated with the interaction of the supporting structure was neglected. The relative displacements and rotations between the cladding panels and the supporting structure needed to be accommodated by the connecting system, owing to the lower stiffness of the connection devices compared to the connected RC precast elements: the cladding panel failure assessed after the Emilia earthquake was clearly related to the failure of the mechanical connections, such as anchor channels, C-shape or L-shape steel profiles (Bournas et al. 2014; Belleri et al. 2016; Colombo et al. 2016).

In recent years, experimental work has been carried out to investigate the performance of cladding-to-structure subassemblies (Colombo et al. 2014; Fischinger et al. 2014; Zoubek et al. 2016a; Pantoli et al. 2016), and design recommendations have been derived accordingly (Belleri et al. 2016 and Colombo et al. 2016), mainly concerning the in-plane behaviour of such systems. In the case of out-of-plane loading, the seismic demand on cladding elements and connections is determined following building code formulae for non-structural elements (clause 4.3.5 in EN 1998-1; clause 13.3 in ASCE 7). Noteworthy, due to the high flexibility of the considered structural typology, it is relevant to account for the cladding-to-structure displacement compatibility because the failure of the connecting system could cause the overturning of the panel. ASCE 7 addresses displacement compatibility in clause 13.3.2.

This paper investigates the out-of-plane performance of column-to-column cladding panels typical of industrial and commercial precast concrete buildings (**Figure 1**). Starting from the available formulae on seismic loads in non-structural components (EN 1998-1, ASCE 7), a new equation is proposed, taking into account the effect of the panels on the structural system. The equation is validated by means of non-linear time-history analyses on selected reference structures. In addition, in order to account for out-of-plane displacement compatibility due to roof flexibility, an analytical procedure is proposed. Design recommendations are made accordingly. The proposed formulation is suitable for the out-of-plane load evaluation of new cladding panels and for the assessment of existing systems. It is worth noting that the design of the cladding panel connections needs to account for both out-of-plane and in-plane loads; the latter are not considered herein as this topic has been already covered in previous research (Belleri et al. 2016).

a.  b. 

Figure 1 - Examples of precast industrial buildings with column-to-column precast cladding panels. a) undamaged panels; b) damaged panels after Emilia earthquakes.

2. Cladding panels: out-of-plane seismic loads

2.1 Current design practice

In the current design practice, the cladding system is typically included as lumped masses in finite element models being the cladding panels categorized as non-structural elements. The out-of-plane seismic loads acting on the panel-to-column connections are evaluated from simplified formulations, typically related to response spectra associated to the supporting structure. The building codes considered herein are ASCE 7 (ASCE 7-10, or newer) and EN 1998-1 (CEN, 2004), the latter being basically derived from ASCE 7.

In EN 1998-1, the inertia load acting on the panel centroid (F_i) takes into account the dynamic amplification associated to parameters such as the relative vertical position of the panel centroid (h_p) compared to the building height (H) and the ratio between the fundamental period of the panel (T_p) and the fundamental period of the building (T_s):

$$F_i = PGA\left[\frac{3(1+h_p/H)}{1+(1-T_p/T_s)^2}-0.5\right]\frac{W_p}{q_a}, \quad (1)$$

where W_p is the panel weight, PGA is the peak ground acceleration as a fraction of g, and q_a is a behaviour factor, which is taken between 1 and 2 for façade elements. For the structural typology being examined, the fundamental period of a precast panel is roughly in the range 0.08-0.5s.

In ASCE 7, the inertia load acting on the panel centroid (F_i) is calculated as:

$$F_i = 0.4\cdot S_{DS}\left[1+2\frac{h_p}{H}\right]\frac{I_p\cdot a_p}{R_p}W_p, \quad (2)$$

where S_{DS} is the spectral acceleration at short period, a_p and R_p are the component amplification and response modification factors respectively; $a_p = 1$, $R_p = 2.5$ for exterior non-structural wall elements and $a_p = 1.25$, $R_p = 1$ for the fasteners of the connecting system. I_p is the component importance factor, ranging from 1 to 1.5. It is worth noting that the amplification factor a_p is intended to capture the ratio T_p/T_s, although, by imposing $a_p = 1$, this formulation does not provide variations of inertia loads due to the change of the fundamental period of vibration of the panel.

Other formulations are available in the literature based on the derivation of floor spectra for multi-storey buildings, either accounting for or disregarding the inelastic behaviour of the lateral force resisting system (Medina et al., 2006; Politopoulos, 2010; Sullivan et al., 2013; Petrone et al. 2015). However, these formulations do not take into considerations the case of non-structural elements at heights below the first storey, such as in the case of column-to-column cladding in single-storey industrial buildings.

EN 1998-1 (§4.3.5.1.2) requires that in the case of non-structural elements of great importance or of a particularly dangerous nature, the seismic analysis should be based on a realistic model of the relevant structures and on the use of appropriate response spectra associated to the supporting structure. The use of modal analysis is also considered in

ASCE 7 as an alternative to **Eq.2**. Another approach is the use of response spectrum analysis, although, in such a case, special care should be placed on the influence of the global force reduction factor; indeed, the load reduction in the cladding panels, compared to an elastic analysis, could be less than what is obtained considering the reduction factor associated to the lateral force resisting system.

Below, a parametric analysis is conducted to check the validity of **Eq.1** and **Eq.2** for the case of column-to-column precast concrete panels on a single-story building; a new simplified procedure is proposed and validated in order to have a more accurate estimation of the out-of-plane loads on such panels and on the connecting system.

2.2 Parametric analysis

To investigate the out-of-plane seismic loads acting on column-to-column cladding panels, a parametric analysis is conducted on a 2D linear elastic structural system constituted by multi-bay frames (**Figure 2**). The columns are pinned to roof beams and each panel is modelled as a linear elastic single degree of freedom system (SDOF) with mass m_p^i and stiffness k_p^i. The mass m_p^i used in the analyses is the panel first modal mass. The analyses consider frames with 2, 4 or 8 columns with equal stiffness. At the top of each column a tributary mass (m_{top}) is placed, whose sum is referred to as roof mass (m_{roof}). 3 or 5 column-to-column cladding panels are placed along the height of each column (being n_p the number of panels on each column, **Figure 2**). Various periods (T_p) and masses (m_p^i) of the panels are considered. The roof mass is selected to obtain a fundamental period of the system in the constant velocity region of the pseudo-acceleration spectrum, indeed the fundamental period of typical industrial and commercial buildings lays in that range. A response spectrum (type 1 spectrum, EN 1998–1) with 4 different soil conditions (A, B, C and D) is considered, and a total of more than 30,000 analyses are performed. **Figure 2** shows an example of the considered structural system: three-bay frame with 4 columns and 5 panels at each side of the frame.

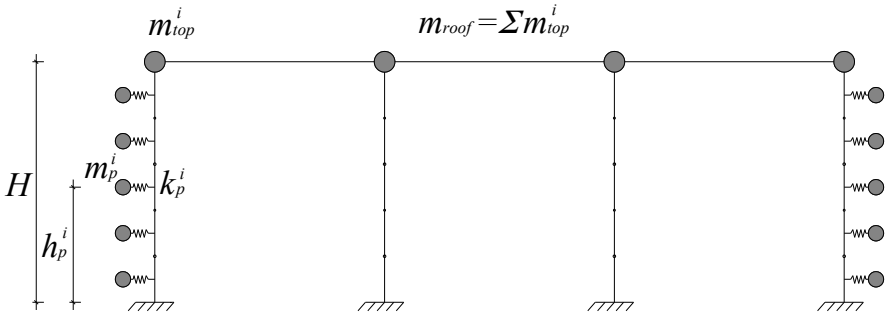

Figure 2 - Structural system considered for the evaluation of the out-of-plane loads on cladding panels

The results of the response spectrum parametric analysis are rearranged as a function of three main dimensionless parameters governing the out-of-plane inertia loads on each cladding panel:

- m_r: the ratio between the total mass of the panels on the two frame ends (mass of each panel multiplied by the total number of panels, 2 n_p) and the roof mass (m_{roof}). It is worth noting that the mass of the panel considered in defining the m_r ratio is the total mass of a single panel (m_p) and not the panel first modal mass used in the analyses (m_p^i).
- T_r: the ratio between the fundamental period of the panel (T_p) and the fundamental period of the system (T_s). T_p is obtained from considering the panel as a simply-supported beam; T_s is obtained from modelling each panel as a lumped mass on the supporting column at a height corresponding to the panel centroid (the spring representing the panel stiffness in **Figure 2** is here removed);
- h_r: the ratio between the vertical position of each panel centroid (h_p) and the column height (H); this ratio identifies the single panel.

The results of the response spectrum analyses are expressed in terms of α (**Figure 3**), which is an amplification factor defined as the ratio between the panel inertia load obtained from the analyses and the load obtained from a linear load distribution (F_a) with top ($F_{a,top}$) and bottom ($F_{a,bot}$) values equal to:

$$F_{a,\,top} = S_a\left(T_s\right)\cdot m_p\,; \quad F_{a,\,bot} = S_a\left(T_p\right)\cdot m_p \tag{3, 4}$$

$S_a(T)$ is the pseudo-acceleration spectral value for a period T, considering a spectrum with 5% relative damping. The decision to refer to such linear load distribution is just aimed at simplifying calculations.

Figure 4 shows the out-of-plane loads on each panel as a function of m_r and T_r in terms of α; the significance of the dashed lines represented in the figure will be explained later. The parametric analyses accounted for a wide range of values for T_r and m_r (0-1.5 and 0.025-1.00 respectively); however, for the geometry distribution of Italian precast concrete industrial buildings (Casotto et al. 2016), the ranges 0.1-0.7 and 0.05-1 should be better considered for T_r and m_r respectively; other values of T_r and m_r could be associated to different structural typologies and cladding systems. The range of interest for the structural typology being considered is represented in each figure with the unshaded area.

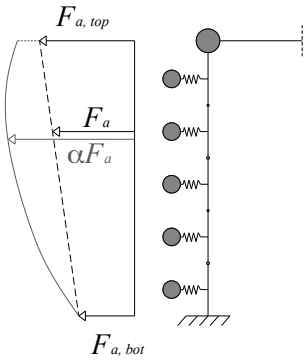

Figure 3 - Actual load distribution on the panels (solid line) and linear distribution (dashed line) considered for the evaluation of the dimensionless load parameter α

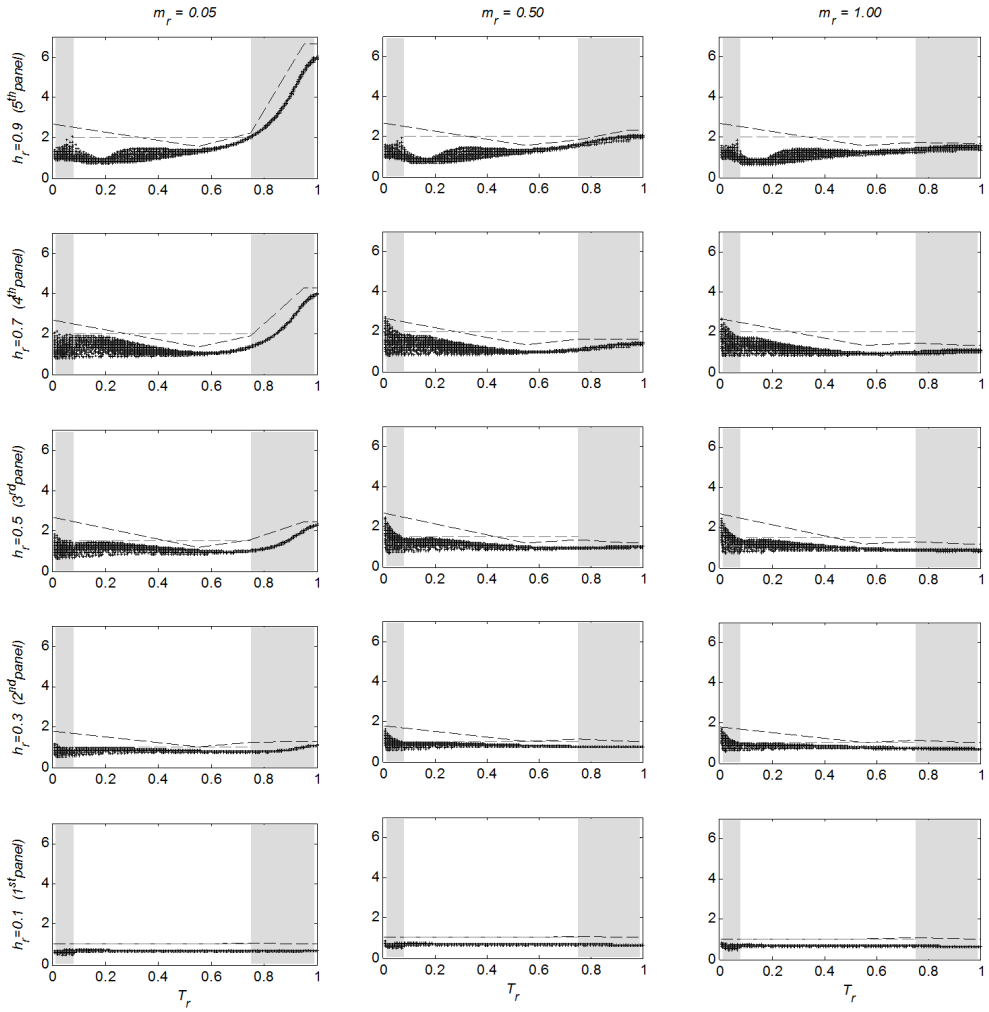

Figure 4 - Loads on each panel in terms of α-value.
Note: range of interest for the considered structural typology in the unshaded area;
the significance of the dashed lines is described in section 2.4 and in Appendix A

Figure 4 shows the results obtained when considering 5 panels along the column's height; similar results are obtained from the case of 3 panels. As expected, a peak value of α in proximity of $T_r = 1$ is observed; such a peak is higher for panels placed at the top of the column and lower for increasing values of the mass ratio (m_r). For T_r lower than 0.5, an increase of α is observed, especially in central panels and for increasing values of m_r. The influence of the number of columns is already accounted for by T_r and m_r. It is important to note that the scatter of the results for T_r values lower than 0.5 is a consequence of the 4 considered spectra (one for each type of soil condition). Indeed, with the structure period's of vibration taken in the constant velocity region and with T_B and T_C (start and end period of the constant

acceleration region) different for each soil type, different amplification factors are obtained for the same T_r when considering different spectra.

2.3 Comparison with current design formulations

The formulations suggested by the codes are compared to the results of the parametric analysis in this section. **Figure 5** shows the minimum values of the ratio between the panel out-of-plane load computed with EN 1998 (**Eq**.**1**) or ASCE 7 (**Eq**.**2**) and the corresponding load obtained from the response spectrum analyses. Values below the unity represent conditions in which the aforementioned equations provide forces smaller than those predicted by the parametric analysis. In the range of interest, the closest fit is provided by **Eq.2** (ASCE 7) for the case of fasteners of the connecting system, especially for the lower panels; **Eq**.**1** (EN 1998-1) is always smaller when considering $q_a = 2$, as commonly adopted in the design practice. In general **Eq.1** (EN 1998-1) with $q_a = 1$ provides higher values than **Eq.2** (ASCE 7). Outside the range of interest, it is worth observing how both formulations could provide unsafe results especially for low values of m_r and values of T_r close to unity (i.e. at resonance). Such conditions, although not necessarily applicable to the cladding system, could refer for instance to other non-structural components as a piping system connected to adjacent columns.

Regarding the cladding panels considered herein, past earthquakes have shown that the failures of such systems typically occur in the connections and fasteners, not in the panels. These failures could be related to different factors, such as low design values of the out-of-plane loading (as applying **Eq.1** with q_a=2), the displacement compatibility in the panels in-plane direction (Belleri et al., 2016; Zoubek et al., 2016a) or as a consequence of the torsion demand arising in the panel, as reported in **chapter 3**.

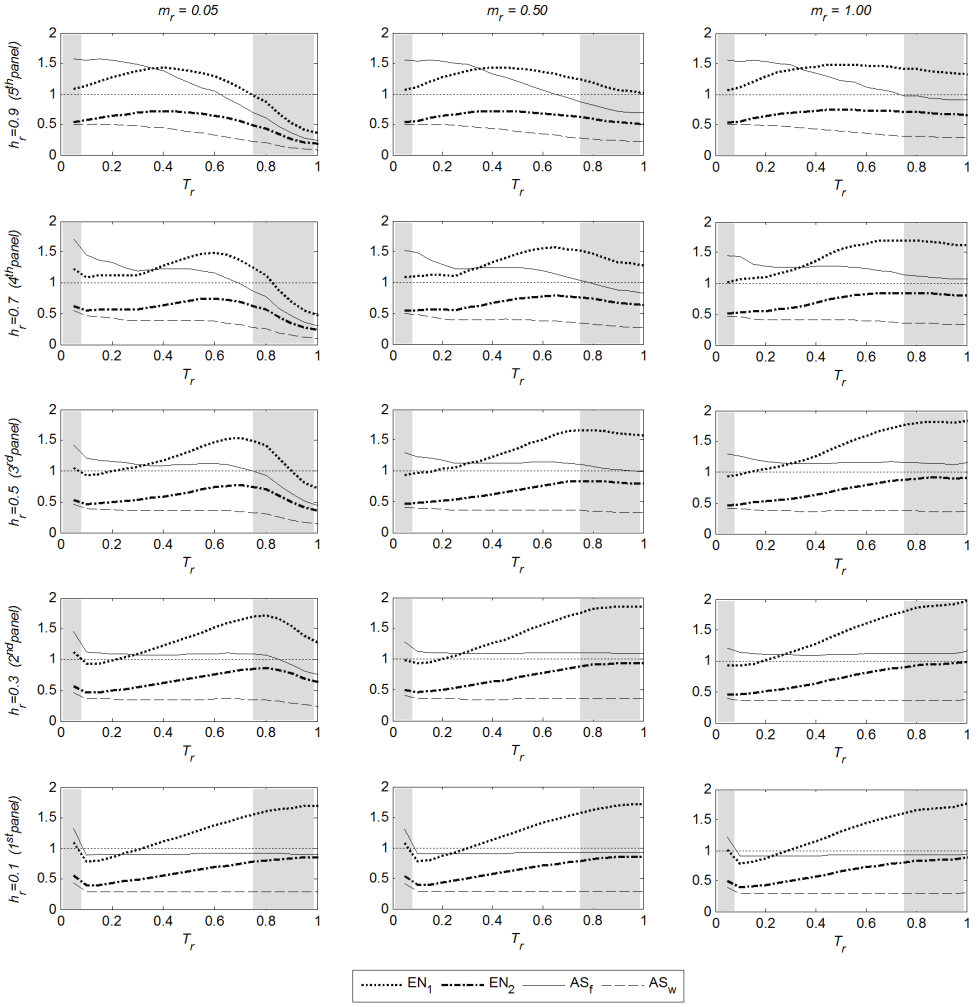

Figure 5 - Minimum ratio between design practice formula and parametric analysis results.
Note: EN_1 and EN_2 consider EN1998-1 formula (Eq. 1) with q_a=1 and q_a=2 respectively;
AS_w and AS_f consider ASCE 7 formula (Eq. 2) for wall element and fasteners respectively, both with I_p=1;
range of interest for the considered structural typology in the unshaded area

2.4 Simplified estimate of the out-of-plane seismic loads

Taking into consideration that the current design equations are not always on the safe side, a simplified procedure is investigated here to better bound the seismic load demand on precast cladding panels of single-storey industrial buildings. The evaluation of the out-of-plane seismic loads on the column-to-column precast cladding panels in precast one-story structures is defined here based on the results of the parametric analysis. A formula of α fitting the results (grey horizontal lines in **Figure 4**) is proposed and represented schematically in **Figure 6:**

$$\begin{cases} \alpha = 1 & for \quad 0 \le h_r \le 0.3 \\ \alpha = 1 + 2.5\left(h_r - 0.3\right) & for \quad 0.3 < h_r \le 0.7 \\ \alpha = 2 & for \quad 0.7 < h_r \le 1 \end{cases} \tag{5}$$

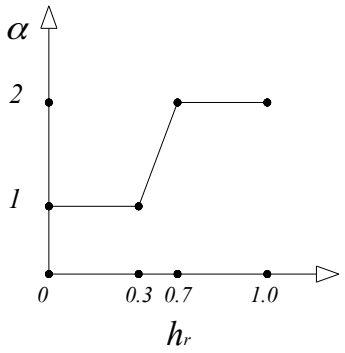

Figure 6 - Simplified linearization of α-value

Eq.5 is independent from T_r and m_r and it is valid for T_r in the range 0.1-0.7 and m_r in the range 0.05-1. Therefore, it is compatible with the precast concrete industrial buildings being considered. The inertia load (F_i) on each panel is obtained by:

1. evaluate $m_r = (2n_p m_p)/m_{roof}$, $T_r = T_p/T_s$ and $h_r = h_p/H$;
2. obtain α from **Eq.5**;
3. calculate the inertia load on the panel (F_i) as:

$$F_i = \alpha \left[F_{a,\,bot} + h_r \left(F_{a,\,top} - F_{a,\,bot} \right) \right] \tag{6}$$

4. calculate the out-of-plane load on each connection ($F_{i,c}$) as:

$$F_{i,c} = F_i / 4 \tag{7}$$

According to the parametric analysis, this procedure has been derived for cladding panels equally distributed along the column's height. In the case of cladding panels with different dimensions but with the same weight density it is still possible to apply the proposed procedure. In the case of relevant differences, more refined analyses should be carried out. It is important to consider that the same issues apply for existing procedures. In the absence of refined analyses, it is suggested to select the highest value among the proposed procedure and the formulae of the building codes.
A refined linearization of α accounting for the influence of T_r and m_r and for values beyond the validity range of **Eq.5** is provided in **Appendix A**.

3. Further considerations

3.1 Influence of plastic hinge development at the column base

The influence of the development of a plastic hinge at the column base has been investigated by means of non-linear time history analyses considering one of the configurations used in the parametric analyses: a single-portal frame with five panels along the height of each column. The plastic hinge is modelled according to the Takeda hysteresis rule (Takeda, 1970). The yield moment is chosen in order to obtain a behaviour factor q equal to 1.5, 2.5 and 4; where q is taken as the ratio between the bending moment obtained from a linear elastic analysis and the yield moment. The ground acceleration is provided by an artificial record; the record is spectrum-compatible with EN 1998–1 type 1 spectrum, soil type A, and a_g=0.35g (ground acceleration on rock), and it is obtained from the SIMQKE-1 algorithm (Venmarcke and Gasparini, 1976).

Figure 7 shows the results of the analyses in terms of load ratio between the inelastic and linear elastic case. The influence of the behaviour factor is relevant especially for the panels in the higher rows and for T_r closed to unity. The difference among the behaviour factors is not relevant in the considered range of T_r, unshaded area in **Figure 7**, and for low values of m_r. The building period is obtained from considering the secant stiffness at yielding of the columns.

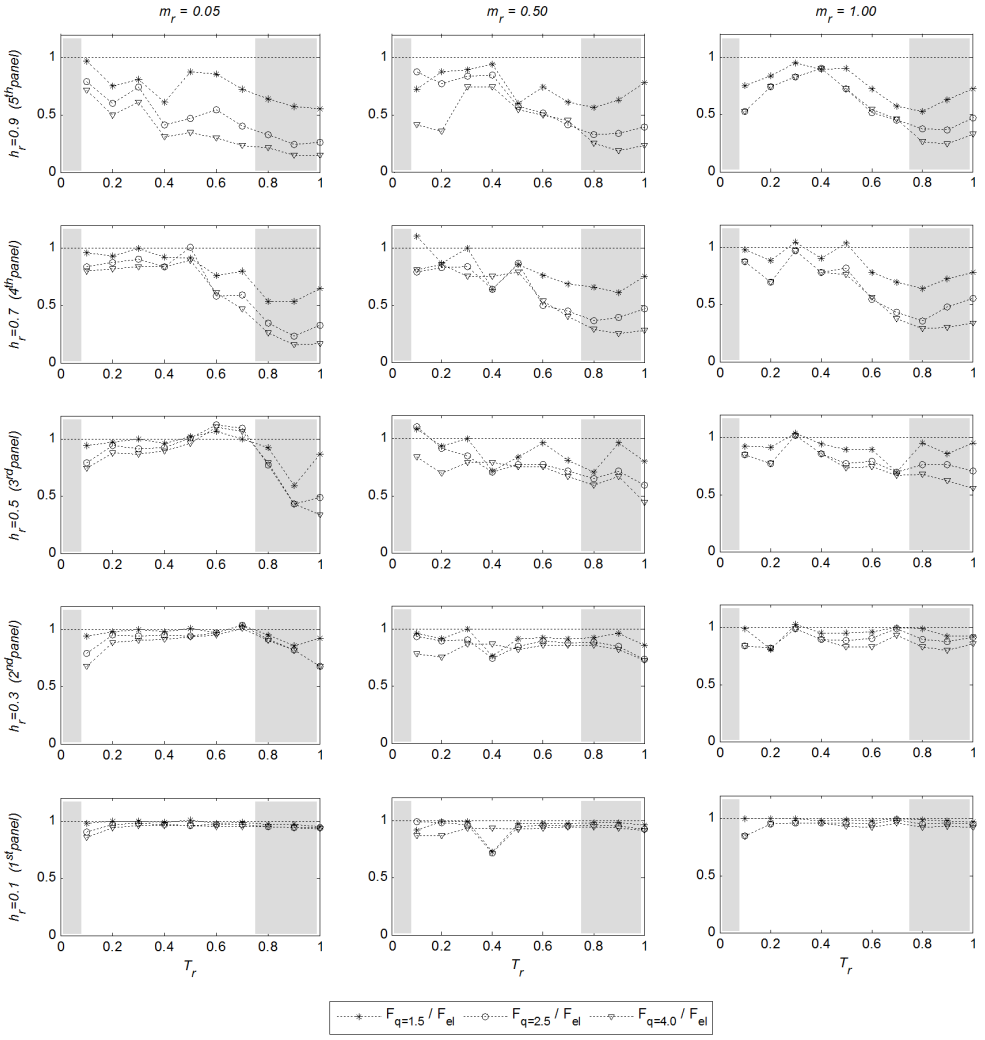

Figure 7 - Ratio between the inertia load in the panel in the inelastic and elastic case.
Note: range of interest for the considered structural typology in the unshaded area

It is essential to note that one-storey precast industrial buildings are characterized by higher flexibility compared to traditional RC building structures, due to the high inter-storey height and to the lateral force resisting system (i.e. cantilever columns fixed at the base). The high flexibility leads to low value of the displacement ductility demand, hence low value of the effective behaviour factor (Belleri et al. 2016). As addressed in EN 1998-1, precast structures generally attain ductility similar to reinforced concrete structures; besides this, owing to the flexibility of the considered structural typology, the design is typically governed by lateral displacement control and code limitations on second order effects rather than material strain limits. Other authors (Fischinger et al. 2014) also addressed the higher relevance of drift and slenderness limitations requirements compared to the behaviour factor in these types of structures.
As a safety measure, it is therefore suggested to evaluate the out-of-plane loads on cladding panels without accounting for the load reduction due to the development of column plastic hinges. In the case of response spectrum analyses this condition is accomplished by considering that the behaviour factor is equal to unity in the cladding out-of-plane load evaluation; this condition is clearly stated in ASCE 7.

3.2 Influence of roof flexibility

The influence of the roof in-plane flexibility on the loads arising in the panel-to-column connections is evaluated herein to provide a further refinement of the proposed formulation. It is worth noting, that these types of flexible roofs are

peculiar of the considered structural typology, where precast and pre-stressed roofing elements with various cross sections (double-T beams, omega-beams or proprietary micro-shed elements) are used to cover long spans. Such elements are connected only to the main girders by means of mechanical connections which provide the horizontal load transfer mechanism for inertia loads. In addition large openings for skylights are quite common, which increase the in-plane roof flexibility. In the case of accessible roofs, as for parking and for multi-storey buildings, the horizontal inertia loads are transferred by diaphragm action engaged by a reinforced concrete topping placed above the roofing elements.
Scotta et al. (2015) observed an increase of the axial loads in the panel connections in the case of flexible roofs. Indeed, these roofs may imply differential deflection of adjacent columns, thereby causing torsion on the cladding panels. The additional loads associated with the panel torsion should be added to the seismic inertia loads considered before.
To evaluate such additional loads, an elastic response spectrum analysis of the whole 3D building is required. In this analysis, each cladding panel is modelled as 2 lumped masses on the supporting columns at a height corresponding to the panel centroid, as is usually carried out in the design practice (**Figure 8a**). Then, the torsion rotation demand (θ) on each panel is determined from the deflected shape of adjacent columns. With reference to **Figure 8b**, θ may be calculated as:

$$\theta = \frac{(x_1 - x_2) - (x_3 - x_4)}{h} \tag{8}$$

where x_1, x_2, x_3, and x_4 are the out-of-plane displacements of the corners of each panel obtained directly from the response spectrum analysis, and h is the height of the panel.
Given θ, the load arising in the panel-to-column connections can be derived taking as reference **Figure 8**. The following assumptions apply:

- θ is equally distributed between the two columns as a consequence of the symmetry in the stiffness of the connections. This implies that $\theta = 4\,\Delta/h$. The panel out-of-plane displacement Δ due to the column deflection may thus be determined.
- The rotational stiffness of the panel-to-column connections is neglected. Therefore the relative rotation between the columns is the only source of additional loads in the panel-to-column connections due to out-of-plane displacement compatibility.

Once Δ is calculated, the additional force in each connection may be directly determined by imposing the equilibrium of the forces on each panel as shown in **Figure 8b**.
From **Figure 8b**, the equilibrium to rotation about axis 3-4 ($F_1 L + F_2 L = 0$) leads to:

$$K_{TC}(\delta_1 - \Delta)L + K_{BC}(\delta_2 + \Delta)L = 0 \tag{9}$$

where δ_i is the axial out-of-plane displacement of the i^{th} connection. K_{TC} and K_{BC} are the axial stiffness of the top and bottom connection, respectively.
The equilibrium to rotation about axis 1-2 ($F_3 L + F_4 L = 0$) leads to:

$$K_{TC}(\delta_3 + \Delta)L + K_{BC}(\delta_4 - \Delta)L = 0 \tag{10}$$

The equilibrium to rotation about axis 2-4 ($F_1 \cdot h + F_3 \cdot h = 0$) leads to:

$$K_{TC}(\delta_1 - \Delta)h + K_{TC}(\delta_3 + \Delta)h = 0 \quad \rightarrow \quad \delta_1 = -\delta_3; \tag{11}$$

Equivalently, considering the rotation about axis 1-3 ($F_2 \cdot h + F_4 \cdot h = 0$) leads to:

$$K_{BC}(\delta_2 + \Delta)h + K_{BC}(\delta_4 - \Delta)h = 0 \quad \rightarrow \quad \delta_2 = -\delta_4; \tag{12}$$

From the rotations associated to the axial displacements of the connections at each side of the panel and the torsion rotation of the panel itself, the following formula is derived:

$$\frac{\delta_1 - \delta_2}{h} - \frac{\delta_3 - \delta_4}{h} + \frac{F_1 \cdot h}{GI_T} L = 0 \tag{13}$$

where G is the shear modulus of concrete and I_T is the torsion constant of the panel.
Substituting **Eq.11**, **Eq.12** and $F_1 = K_{TC}(\delta_1 - \Delta)$ into **Eq.13** gives:

$$2\delta_1 - 2\delta_2 + \frac{K_{TC}(\delta_1 - \Delta) \cdot h^2}{GI_T} L = 0 \tag{14}$$

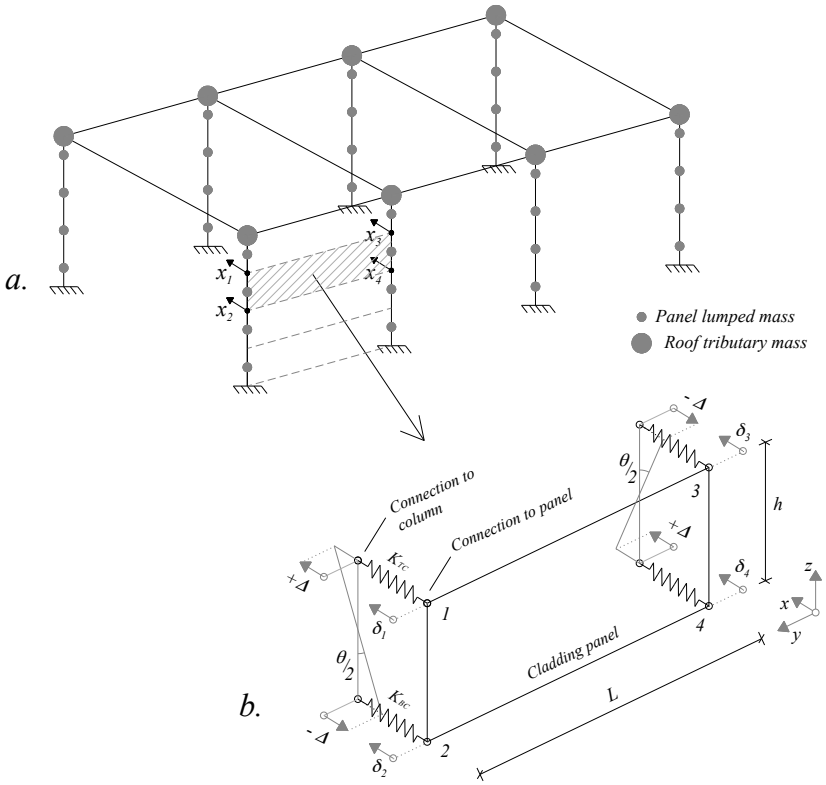

Figure 8 - Model used to evaluate panel rotation (a);
scheme of the cladding panel connections system (b).

Considering the system constituted by **Eq.9** and **Eq.14** the following formulae for δ_1 and δ_2 are finally obtained:

$$\delta_1 = \frac{\Delta \frac{Lh^2}{GI_T} K_{BC} K_{TC} - 2\Delta\left(K_{BC} - K_{TC}\right)}{2K_{TC} + 2K_{BC} + \frac{Lh^2}{GI_T} K_{BC} K_{TC}} \tag{15}$$

$$\delta_2 = \frac{-\Delta \frac{Lh^2}{GI_T} K_{TC}{}^2 - \Delta\left(K_{BC} - K_{TC}\right)\left(2 + \frac{Lh^2}{GI_T} K_{TC}\right)}{2K_{TC} + K_{BC}\left(2 + \frac{Lh^2}{GI_T} K_{TC}\right)} \tag{16}$$

δ_3 and δ_4 are obtained from **Eq.11** and **Eq.12**. The force in each connection is thus:

$$F_1 = -F_3 = K_{TC}(\delta_1 - \Delta); \quad F_2 = -F_4 = K_{BC}(\delta_2 + \Delta) \tag{17; 18}$$

As mentioned before, such forces represent additional loads, which need to be added to the load on each connection obtained with **Eq.7**. Such load increase could be up to 4 times what predicted by **Eq.7**, which is highlighted in the following section.

4. Procedure validation: numerical simulations and design implications

In order to validate the proposed formulations, a case study resembling a typical industrial precast building is selected. The structural layout is shown in **Figure 9**. Cantilever columns (7.2m tall) constitute the lateral force resisting system; the columns are pin-connected at the top by a gutter beam (cross section 40x80 cm). The seismic design complies with EN 1998–1 type 1 elastic spectrum, soil type A and a peak ground acceleration (PGA) of 0.35 g at the design basis earthquake limit state. Each column has a square cross-section (0.6x0.6m) reinforced with 16 longitudinal 18mm diameter bars, equally distributed along the edges. The concrete cover is 40mm. The columns support 12 cladding

panels along the building longitudinal side. The cladding panel geometry is 2.4x8.0x0.2m. The roof tributary mass at the top of each column is 33,000kg and 66,000kg for the corner and inner columns respectively. Non-linear time history (NLTH) and response spectrum (RS) analyses (MidasGEN, 2012) are carried out on the lateral frame presented in **Figure 9** considering the out-of-plane direction. The NLTH analyses are conducted considering the same artificial ground motion of section 3.1 and accounting for large displacements. Each panel is modelled as plate elements with a mesh of 4 by 8 elements. The panel mass is directly included in the model by assigning a mass density to the corresponding plate element. The columns, fixed at the base and pin-connected to the gutter beam, are modelled by means of non-linear fibre elements with concrete strength equal to 40MPa and yield stress of the steel reinforcement equal to 450MPa.

The considered panel-to-column connections are constituted by bearing elements at the bottom and retaining elements at the top (**Figure 10**) as reported in Belleri et al. (2016). Such connections have been selected for demonstration purpose. The formulations presented in the previous chapters are also applicable to other types of mechanical connections, provided that the appropriate connection stiffness is derived. Referring to the selected case study, the bottom bearing connection is made of a rectangular steel element placed into a steel pocket inside the column during erection; a supporting bolt (M24 class 8.8) is placed at the end of the plate to adjust for vertical tolerances. The top retaining connection is made by a vertically oriented anchor channel (cold formed channel, grade S250GD) embedded in the column, a slotted-plate anchored into the panel (S235), and a connecting T-bolt (M16, class 5.6) with washers and nuts. The vertical orientation of the anchor channel is intended to accommodate vertical tolerances, while the horizontal slot in the slotted-plate is intended to accommodate lateral tolerances.

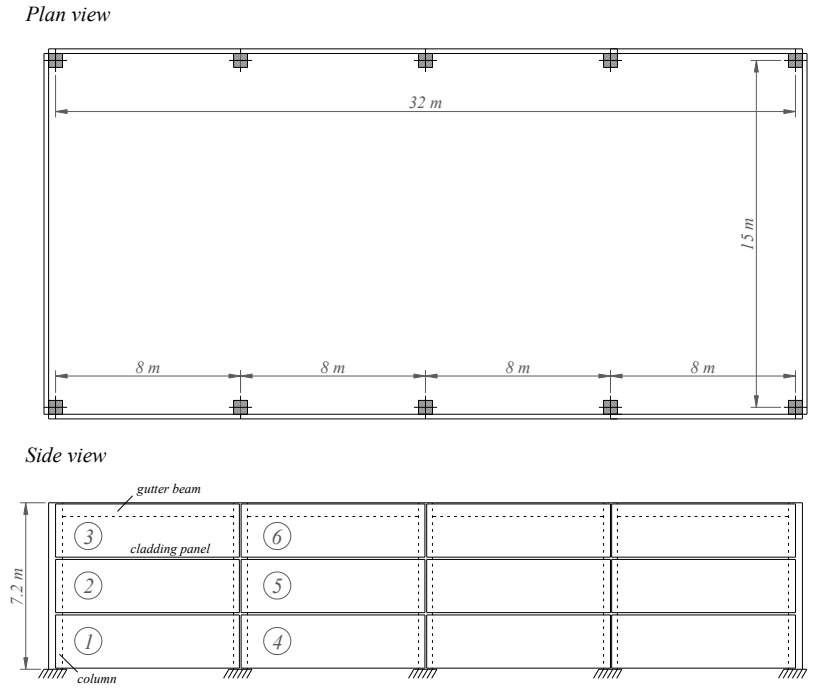

Figure 9 - Case study geometry.

As regards the bottom connection, the in-plane and out-of-plane force-displacement relationships are modelled by means of springs with a symmetric elasto-plastic hysteresis: the stiffness is evaluated considering the supporting bolt as a cantilever beam with a horizontal load at the top; the yielding load is associated with the flexural capacity of the bolt.

The top connection is modelled as a roller in the panel in-plane direction; the out-of-plane force-displacement relationship is modelled by means of an asymmetric elasto-plastic hysteretic spring. Such asymmetry is associated with the different behaviour of the anchor channel in the case of compressive or tensile loads. For tensile loads, the T-bolt pulls the anchor channel lips directly, while compressive loads are transferred to the anchor channel sides by the washer and the nut. Considering that the slotted-plate, the bolt, and the anchor channel are connected in series, the failure of the weakest component governs the connection capacity; the equivalent stiffness of the connection assembly (k_{eq}) is related to the stiffness of each component by:

$$1/k_{eq} = 1/k_{sl} + 1/k_b + 1/k_{ac} \tag{19}$$

where k_{sl} is the out-of-plane stiffness of the slotted-plate, k_b is the axial stiffness of the bolt and k_{ac} is the out-of-plane stiffness of the anchor channel.

In the case of tensile loads acting on the anchor channel (**Figure 11a**), the out-of-plane capacity is obtained following the procedure used for anchorages in concrete, as for instance reported in Eligehausen et al. (2006) or in product approvals. In general, the out-of-plane stiffness can be estimated by considering the bending stiffness of the channel

between two anchors. In the present case study, the configuration associated with the highest axial stiffness of the connection is analysed, taking into account that the out-of-plane stiffness governs the load increase due to torsion of the panel. Such configuration is associated with a T-bolt placed in correspondence to an anchor point. Accordingly, the development of yield lines in the anchor channel lips (**Figure 11b**) is assumed to govern the anchor channel performance. The stiffness and capacity of this configuration is derived following the procedure reported in Belleri et al. (2016). It is worth mentioning that in the case of out-of-plane loads, both the channel lips are subjected to tensile loads, while the aforementioned formulation (Belleri et al. 2016) considers the load acting on a single lip. In the case of compressive loads (**Figure 11c**), the bending of the washer is herein considered according to the static scheme of **Figure 11d**. Other static schemes can be selected due to different configurations or as a result of experimental tests. **Table 1** reports the stiffness and the capacity of each component (calculations in **Appendix C**) along with the characteristics of the elasto-plastic springs used in the non-linear time history analyses.

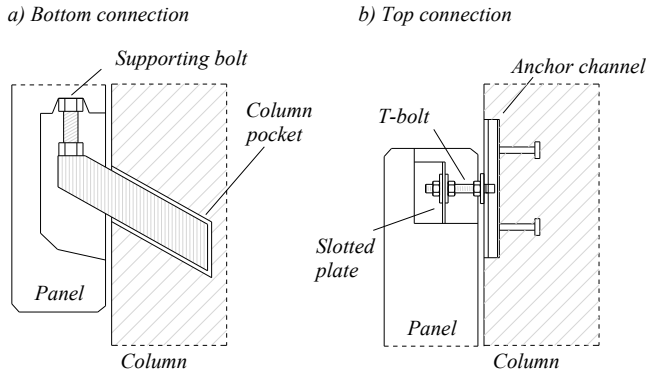

Figure 10 - Considered bottom (a) and top (b) panel-to-column connections.

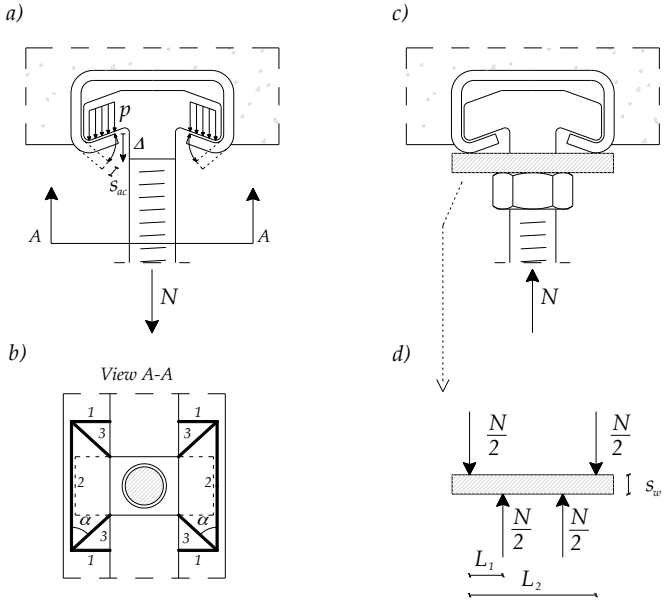

Figure 11 - Top connection anchor channel behaviour for tensile (a, b) and compression (c, d) loads.

Two sets of analyses are carried out to account for possible in-plane stiffness of the roof: rigid diaphragm and flexible diaphragm. In the former case, the columns are forced to have the same out-of-plane top displacement. In the latter case, the roof in-plane stiffness is governed by the gutter beam, therefore resembling a condition in which the roof elements are not mutually interconnected and behave like truss elements. **Table 1** reports the mechanical characteristics of the connections. An additional finite element model is considered. Such model, referred to as point mass model, represents the typical mesh used in the design practice: each panel is modelled directly with point masses fixed to the supporting columns at a height corresponding to the panel centroid (as in **Figure 8a**). This model is used to evaluate the torsion rotation demand on the panel by means of elastic response spectrum analyses (RS-PM), as reported in **Table 2**. The panel rotation demand is obtained from combining the rotation associated with each mode by following the SRSS rule. In general, this procedure provides higher estimates than considering directly the displacements obtained from a global response spectrum response (**Table 2**). This is particularly evident for the case of rigid diaphragm.

Table 1 Hysteretic model of each connection.

Connection	Component	Stiffness (kN/m)	Capacity (kN)	Hysteretic model
Bottom	Supporting bolt	49,977	20.3	K_{BC} = 49,977 kN/m; $F_{y,BC}$ = 20.3 kN
Top	Slotted Plate	141,590	20.0	Tension: $K_{TC}^{tension}$ = 44,831 kN/m; $F_{y,TC}^{tension}$ = 16.4 kN Compression: $K_{TC}^{compression}$ = 63,847 kN/m; $F_{y\,TC}^{compression}$ = 19.5 kN
	Bolt	412,125	47.1	
	Anchor channel (tension)	78,022	16.4	
	Anchor channel (compression)	161,988	19.5	

Table 2 Torsion rotation of the panel.
Note: RS-PM = results from the elastic response spectrum analysis with *point mass* model;
NLTH = results from non-linear time history analyses;
* rotation demand evaluated from global response spectrum response;
** rotation demand evaluated for each mode and then applying SRSS.

Panel id. (**Fig. 9**)	**Torsion rotation of the panel (10^{-3} rad)**					
	Rigid diaphragm			**Flexible diaphragm**		
	RS-PM*	RS-PM**	NLTH	RS-PM*	RS-PM**	NLTH
1	0.07	0.43	0.84	3.9	4.1	7.5
2	0.03	0.17	0.25	9.6	9.1	10.5
3	0.09	0.63	0.87	11.7	11.0	11.1
4	0.02	0.63	0.21	1.3	1.3	6.5
5	0.01	0.24	0.07	2.6	3.2	9.8
6	0.02	0.90	0.24	3.5	4.0	10.2

Table 3 shows the results of the response spectrum (RS) and non-linear time history (NLTH) analyses in the case of rigid diaphragm, as well as the predicted out-of-plane loads in the connections (**Eq.7**) and the design load obtained from **Eq.1** (EN 1998-1) and **Eq.2** (ASCE 7). It can be observed that **Eq.7** is generally able to capture the out-of-plane loads on the panel-to-column connections, although under-estimation occurs in the first row of panels (Panel 1 and 4 in **Figure 9**). Conservative estimations are obtained from including the panel torsion (**Eq.7** plus **Eq.17-18**). It is important to note that **Eq.1** (EN 1998–1) with $q_a = 2$, as typically adopted in the design practice, leads to not conservative predictions. In the case of **Eq.1** with $q_a = 1$, the load estimated in the most loaded panel is conservative. Besides this, such value is associated with the upper panels while the most loaded panels are located in the bottom row, as predicted by the NLTH analysis. Similar considerations apply to ASCE 7: **Eq.2** provides loads lower than the demand for "wall elements" and loads close to EN 1998–1 ($q_a = 1$) for "fastener of the connecting system".
It is interesting to note that **Table 3** show that the largest forces are not acting on the panels in the top row, as it would be expected by applying building code formulae. This is in agreement with the results of the parametric analysis (Eq. 7 column in **Table 3**). To further clarify this result, let us consider a horizontal cladding panel whose out-of-plane period of vibration is in the constant acceleration region of the spectrum, and let us consider the elastic case for demonstration purpose; given these premises, if the panel is attached at the bottom of the column it will experience a higher demand compared to the same panel attached at the top of the column, indeed in the former case the panel experiences the maximum spectral acceleration, while in the latter case a lower out-of-plane acceleration can be found because the panel and the building behave as springs in series and the resulting period of vibration elongates.
Table 4 shows the analyses results in the case of flexible diaphragm. The results show that all the connections exhibit plastic behaviour as a consequence of the panel torsion rotation, as foreseen by the proposed formulation (**Eq.7** plus **Eq.17-18**). Such inelastic behaviour could lead to a premature failure of the connections and possible panel out-of-plane overturning. **Eq.1** (EN 1998–1) and **Eq.2** (ASCE 7) are not able to capture the additional loads due to roof flexibility, leading to substantial underestimation of the connection demand in the case of in-plane flexible roofs. Additional analyses were carried out to evaluate the influence of the anchor channel compression capacity, by assuming an elastic behaviour in compression of the top connection. An average 16% load increase in the panel connections was observed.

Table 3 Maximum axial load in panel connections for the rigid diaphragm case.
Note: RS = results from elastic response spectrum analyses;
NLTH = results from non-linear time history analyses;
* Force in each connection obtained diving **Eq.1-2** by 4;

Panel connection		**Force in the connection (kN)**							
Panel id. (**Fig. 9**)	Top or bottom	RS	NLTH	Eq.7	Eq.7 + Eq.17,18	EN-1998 * (q_a=1)	EN-1998 * (q_a=2)	ASCE 7 * wall element	ASCE 7 * fastener
1	TC	16.6	18.8	18.3	19.9	12.4	6.2	4.5	14.0
	BC	15.9	18.7	18.3	19.9	12.4	6.2	4.5	14.0
2	TC	13.5	14.0	19.5	20.1	17.2	8.6	6.7	21.0
	BC	13.9	14.5	19.5	20.1	17.2	8.6	6.7	21.0
3	TC	7.4	7.5	15.3	17.6	21.8	10.9	9.0	28.0
	BC	7.7	7.6	15.3	17.6	21.8	10.9	9.0	28.0
4	TC	15.5	16.6	18.3	20.6	12.4	6.2	4.5	14.0
	BC	14.3	16.1	18.3	20.6	12.4	6.2	4.5	14.0
5	TC	15.8	16.5	19.5	20.4	17.2	8.6	6.7	21.0
	BC	15.5	16.5	19.5	20.4	17.2	8.6	6.7	21.0
6	TC	6.9	6.8	15.3	18.6	21.8	10.9	9.0	28.0
	BC	7.7	8.3	15.3	18.6	21.8	10.9	9.0	28.0

Table 4 Maximum axial load in panel connections for the flexible diaphragm case.
Note: RS = results from elastic response spectrum analyses;
NLTH-el = results from non-linear time history analyses with elastic connections;
NLTH-in = results from non-linear time history analyses with inelastic connections;
* Force in each connection obtained diving **Eq.1-2** by 4;

Panel connection		**Force in the connection (kN)**					
Panel id. (**Fig. 9**)	Top or bottom	RS	NLTH–el	NLTH–in	Eq.7 + Eq.17,18	EN 1998 * (q_a=1)	ASCE 7 * fastener
1	TC	23.4	39.9	19.5	33.2	12.2	14.0
	BC	22.9	39.9	20.6	33.2	12.2	14.0
2	TC	40.8	47.3	19.5	52.3	17.0	21.0
	BC	40.8	48.6	21.1	52.3	17.0	21.0
3	TC	47.6	48.9	19.5	55.1	21.6	28.0
	BC	47.7	49.1	21.0	55.1	21.6	28.0
4	TC	18.4	29.8	19.5	23.0	12.2	14.0
	BC	18.0	30.3	20.3	23.0	12.2	14.0
5	TC	27.9	45.5	19.5	30.9	17.0	21.0
	BC	27.7	46.0	20.6	30.9	17.0	21.0
6	TC	29.1	44.4	19.5	29.4	21.6	28.0
	BC	29.4	45.2	20.5	29.4	21.6	28.0

Finally, a NLTH analysis with elastic panel-to-column connections (NLTH-el) is carried out. The results (**Table 4**) are compatible with the proposed formulation (**Eq.7** plus **Eq.17-18**) in the case of side panels (panels 1-3 in **Figure 9**). Loads higher than what predicted by all the investigated formulations are obtained in the case inner panels (panels 4-6 in **Figure 9**). Such a difference is related to panel rotations higher than predicted (**Table 2**) due to both asynchronous displacements of adjacent columns and different ductility levels developed by the plastic hinge at the base of the

columns. This behaviour is not captured by response spectrum analyses. To limit the uncertainties associated with these phenomena it is possible to increase the out-of-plane displacement capacity of the connections, as, for instance, adding cup springs at each side of the retaining slotted plate of the top connection (**Figure 12**).

Based on the obtained results, the following design procedure is suggested:
Step 1 - Evaluate the out of plane loads on the panels by means of **Eq.7**; take the maximum value for the top and bottom connections. In the case of cladding panels with different dimensions but with the same weight density it is still possible to apply the proposed procedure. In the case of relevant differences, it is suggested to select the highest value among the proposed procedure and the formulae of the building codes.
Step 2 - Evaluate the torsion rotation demand on the panels by means of an elastic response spectrum analysis. In this regard, it is possible to adopt a finite element model with panels modelled as point masses placed on the columns at a height corresponding to the panel centroid.
Step 3 - Use the maximum rotation found in Step 2 to get the additional loads in the top and bottom connections by means of **Eq.17-18**. As a starting point, use the stiffness of the connections able to carry the loads found in Step 1. This step may require iterations.
Step 4 - Design all the bottom and top connections, independently by the location of the panel, according to the sum of the loads obtained in Step 1 and Step 3. Repeat from Step 3 to account for changes in the connection stiffness.
Step 5 - Limit the load demand arising from panel torsion rotation (Step 3). This can be accomplished by decreasing the axial stiffness and by increasing the axial displacement capacity of the top connections. A possible solution is depicted in **Figure 12**.
Step 6 - Avoid the overturning of existing cladding panels if failure of the connections occurs. The same retrofit strategies presented in Belleri et al. (2016), Zoubek et al. (2016b), Dal Lago et al. (2017) among others are appropriate as back-up systems.

It is worth noting that the sealant applied between panels for aesthetical reasons and to prevent air flow can alter the load path of seismic actions. Indeed, experimental tests (Dal Lago et al. 2017) conducted on precast panels under in-plane deformations showed that the silicone joints influence the seismic performance at the serviceability limit state and increase the load demand on the panel connections, although they are not suitable to sustain the relative displacements typically associated with the ultimate limit state. The influence of sealant was not considered herein.

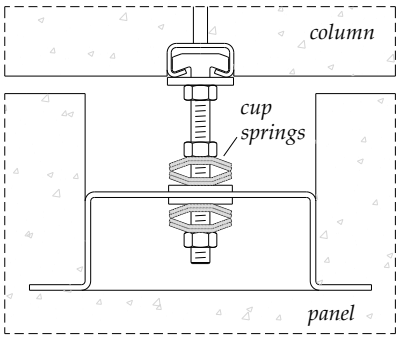

Figure 12 - Increase of axial deformation capacity of top connections by means of cup springs.

5. Conclusions

The paper investigated the out-of-plane seismic response of column-to-column precast cladding panels in the case of single-storey industrial and commercial precast buildings. Parametric finite element analyses were carried out by considering the ratio of the panel-to-structure fundamental period of vibration, the ratio of the panel-to-structure mass, and the relative position of the panel centroid with respect to the column height. For the considered structural typology, the formulations available in building codes (EN 1998-1, ASCE 7) provided conservative values of inertia loads in just two cases: in ASCE 7, when the formulation for the fasteners of the connecting system is considered; in EN 1998-1, when no reduction factor for the non-structural component is adopted. For other structural typologies, existing formulations could lead to not conservative estimations. Given the poor correspondence between the current design formulations and the parametric analyses, a procedure for the estimation of the seismic inertia loads on cladding panels was derived. The proposed procedure required a simplified model of the structure, the same model used in the response spectrum analyses carried out in the design practice, and it allowed the calculation of the panel loads with a direct empirical formula. Such equation was derived considering a simplified 2D model with the panels modelled as single degree of freedom systems. This procedure did not consider the roof flexibility.

Some other aspects were then investigated in order to refine the out-of-plane load estimation. Plastic hinge development at the column base showed to have a little influence. However, roof in-plane flexibility might play an important role in determining the loads in the panel-to-column connections. Indeed, the torsion arising in the panels associated with differential displacements of adjacent columns leads to additional loads in the connections, which need to be added to the out-of-plane inertia loads. An improvement to the previous procedure was thus derived to account for such loads. This load contribution is not accounted for in existing simplified formulations.

The proposed formulations were derived considering: single-storey precast buildings, column-to-column cladding panels, panels with the same geometry and equally distributed along the building height, and a fundamental period of the structure in the constant velocity region of the pseudo-acceleration spectrum. The latter is typical of the structural typology being examined. In the case of cladding panels with different dimensions but same weight density, it is still possible to apply the proposed formulation. In the case of relevant differences, more refined analyses should be carried out. It is important to note that the same issues apply for existing building code formulations. In the absence of refined analyses, it was suggested to select the highest value among the proposed formulation and the building codes equations.

The proposed procedure was validated by means of non-linear time history analyses. A case study resembling a typical precast industrial building with column-to-column cladding panels was selected. In general, a positive correspondence was found between the numerical and the predicted results. In some cases, the rotation demand on the panels was more than expected due to the asynchronous displacements of adjacent columns and to the different ductility level developed by the plastic hinges of adjacent columns; as a consequence, the load demand in the connections increased.

From the previous findings, some practical design recommendations were made. In particular, it was suggested to design all the bottom and top connections according to the maximum demand (i.e. out-of-plane inertia loads plus loads arising from panel torsion rotation) independently by the location of the panel. Moreover, to limit the load demand arising from panel torsion rotation, an increase of the elastic out-of-plane displacement capacity of the top connection was suggested. It that regard, a possible solution was provided. Finally, it is important to note that the proposed formulations are suitable for the out-of-plane load evaluation of new cladding panels and for the assessment of existing systems. As regards cladding panel connections, the design needs to account for both out-of-plane and in-plane loads. The latter are not considered herein as this topic has been already covered in previous research.

Acknowledgements

The financial support of the ReLUIS project (Italy) is gratefully acknowledged. The opinions, findings, and conclusions expressed in the paper are those of the authors.

APPENDIX A

A refined formula of α is provided here. The fitting of the parametric analysis results is represented in black dashed lines in **Figure 4**. Four regions are identified (**Figure A1**) delimited by five values of T_r ($T_{r\,1}$= 0, $T_{r\,2}$= 0.55, $T_{r\,3}$= 0.75, $T_{r\,4}$= 0.95, and $T_{r\,5}$= 1). α is assumed to vary linearly as a function of T_r in each region j:

$$\alpha = \alpha_j + T_r \frac{\alpha_{j+1} - \alpha_j}{T_{r\,j+1} - T_{r\,j}} \tag{A.1}$$

The values of α delimiting each region (α_j and α_{j+1}) are obtained by means of linear least squares and further increased by 10% in order to cover all the data. The results are expressed as a function of h_r and m_r:

$$\alpha_1 = \begin{cases} 1.0 & for \quad h_r < 0.1 \\ 3.75 \cdot h_r + 0.63 & for \quad 0.1 \le h_r < 0.5 \\ 2.5 & for \quad 0.5 \le h_r < 0.9 \end{cases}$$

$$\alpha_2 = 1 + 0.83 \cdot h_r^2 - 0.1 \cdot h_r \tag{A.2}$$

$$\alpha_3 = -0.9 \cdot h_r \cdot m_r + 1.7 \cdot h_r + 0.7$$

$$\alpha_4 = \alpha_5 = c \cdot m_r{}^d$$

Where $c = 1.87 \cdot h_r^2 - 0.68 \cdot h_r + 0.78$, and $d = 0.64 \cdot h_r^2 - 1.23 \cdot h_r + 0.12$. The minimum α allowed in all the regions corresponds to α_2.

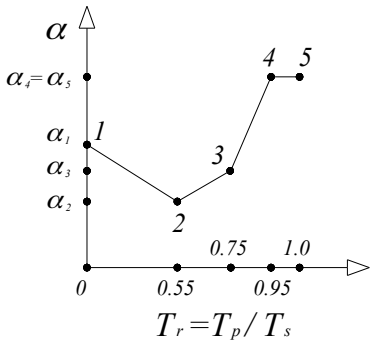

Figure A1 - refined linearization of α-value

The updated procedure to obtain the inertia load (F_i) on each panel is:

1. evaluate $m_r = (2n_p m_p)/m_{roof}$, $T_r = T_p/T_s$ and $h_r = h_p/H$;
2. select the region (**Figure A1**) which T_r belongs to;
3. evaluate α_j and α_{j+1} corresponding to the delimiting points of the selected region (**Eq**. **A.2**);
4. get the appropriate α from **Eq**. **A.1**;
5. calculate the inertia load on the panel (F_i) as:

$$F_i = \alpha \left[F_{a,\,bot} + h_r \left(F_{a,\,top} - F_{a,\,bot} \right) \right] \tag{A.3}$$

6. calculate the out-of-plane load on each connection ($F_{i,c}$) as:

$$F_{i,c} = F_i / 4 \tag{A.4}$$

APPENDIX B

This appendix reports the stiffness and the capacity of the top and bottom connections considered in the non-linear time history analyses. Regarding the bottom connection (**Figure 11a**), the stiffness and the capacity are related to the supporting bolt considered as a cantilever beam with a horizontal load applied at the free end. The bolt is M24, class 8.8 (f_y = 640MPa), and 40mm long (L_b). The lateral load ($F_{y,BC}$) associated with the development of the plastic moment at the base of the bolt is

$$F_{y,\,BC} = f_y \cdot W_{PL} / L_b = 20.3kN \tag{B.1}$$

The lateral stiffness is:

$$K_{BC} = 3EI / L_b^3 = 49{,}977kN \tag{B.2}$$

The top connection (**Figure 11b**) is characterized by a vertical anchor channel (cold formed channel, grade S250GD) embedded in the column, a slotted-plate anchored into the panel (S235) and a connecting T-bolt (M16, class 5.6, f_y = 300MPa) with washers and nuts. Being such elements in series, the connection capacity is governed by the capacity of the weakest element and the stiffness is evaluated according to elements in series.
The capacity of the T-bolt is evaluated as the axial force at yield, $F_{y,b}$=47.1kN, being the buckling load equal to 159kN; the axial stiffness is $k_b = EA/L_b$ = 412,125kN/m, where L_b is 80mm.
The capacity of the slotted-plate (S235, f_y = 235MPa) is evaluated considering a fix-end plate with equivalent cross-section (8mmx60mm) and length L_{sl} = 90mm. The maximum load is associated with the plate flexural capacity $F_{y,sl}$ = 8 M_y / L_{sl} = 20.0kN. The slotted-plate stiffness is k_{sl} = 192 EI/L_{sl}^3 = 141,590kN/m.
Regarding the anchor channel, the case of tensile and compressive load is distinguished. For tensile loading, the capacity is evaluated as twice (2 anchor channel lips) the formulation presented in Belleri et al. (2016) in accordance to the yield-line mechanism presented in **Figure 11b**.

$$F_{y,ac}^{\ tension} = 2\left[f_y \cdot s_{ac}^{\ 2} \cdot \left(4 + \frac{i}{2t}\right)\right] = 16.4kN \tag{B.3}$$

where f_y = 250MPa is the yield stress of the anchor channel, s_{ac} = 2.5mm is the thickness of the lip (cold formed), i = 20mm is the thickness of the head of the connecting bolt and t = 8mm is the contact length between the channel lip and the T-bolt. In the case of tensile loads acting on the anchor channel, the out-of-plane capacity is obtained following the procedure derived for anchorages in concrete, as for instance reported in Eligehausen et al. (2006) or in product approvals; the out-of-plane stiffness could be generally estimated by considering the bending stiffness of the channel between two anchors. In the present case study, the worst configuration in terms of axial stiffness of the connection is considered, being the out-of-plane stiffness governing the load increase due to panel's torsion; such configuration is associated with a T-bolt in correspondence to an anchor point.
The anchor channel stiffness is:

$$k_{ac}^{\ tension} = F_{y,ac}^{\ tension} / \Delta_{tot} = 78'022\frac{kN}{m} \tag{B.4}$$

where Δ_{tot} is the yield displacement of the lip due to the applied load. Δ_{tot} is equal to 0.21mm and it is evaluated according to Belleri et al. (2016) (h = 22mm, t = 8mm, b_{eq} = 35.2mm, s = 2.5mm, i = 20mm, E = 210,000MPa).
In the case of compressive loading, the capacity of the anchor channel is related to the washer according to the scheme of **Figure 11d**. An equivalent plate (39mm x 8mm) is considered neglecting the hole of the washer. The load associated with the flexural capacity of the cross-section is

$$F_{y,ac}^{\ compression} = 2 \cdot \frac{N}{2} = 2\frac{M_y}{L_1} = 2\frac{f_y \cdot L_p s_w^2 / 4}{L_1} = 19.5kN \tag{B.5}$$

where f_y = 235MPa, L_p = 39mm is the width of the washer equivalent plate, s_w = 8mm is the thickness of the plate and L_1 = 15mm is the distance represented in **Figure 11d**.
The anchor channel stiffness is:

$$k_{ac}^{\ compression} = \frac{48 \cdot EI}{L_1(3L_2^2 - 4L_1^2)} = 161{,}988\frac{kN}{m} \tag{B.6}$$

where L_2 = 51mm is the distance represented in **Figure 11d**.
Finally, the equivalent stiffness of the top connection is obtained from Eq. 18 as $K_{TC}^{\ compression}$ = 63,847kN/m and $K_{TC}^{\ tension}$ = 44'831kN/m. The capacity of the top connection is associated with the capacity of the anchor channel for both tensile ($F_{y,TC}^{\ tension}$ = 16.4 kN) and compressive loading ($F_{y\,TC}^{\ compression}$ = 19.5 kN).

REFERENCES

ASCE 7-10 (2010) Minimum Design Loads for Buildings and other Structures, American Society of Civil Engineers, Virginia, USA

Ambraseys N, Smit P, Douglas J, Margaris B, Sigbjornsson R, Olafsson S, Suhadolc P, Costa G (2004) Internet-site for European strong-motion data. Bollettino di Geofisica Teorica ed Applicata, 45(3), 113–129

Arnold C (1989) Cladding design: architectural trends and their influence on seismic design. Proceedings: Architectural Precast Concrete Cladding – It's Contribution to Lateral Resistance of Buildings. PCI, November 8-9, Chicago

Belleri A (2017) Displacement based design for precast concrete frames with not-emulative connections. Engineering Structures, doi: 10.1016/j.engstruct.2017.03.020

Belleri A, Riva P (2012) Seismic performance and retrofit of precast concrete grouted sleeve connections. PCI Journal, 57(1):97-109

Belleri A, Brunesi E, Nascimbene R, Pagani M, Riva P (2014a) Seismic Performance of Precast Industrial Facilities Following Major Earthquakes in the Italian Territory. J. Perform. Constr. Facil., doi:10.1061/(ASCE)CF.1943-5509.0000617

Belleri A, Torquati M, Riva P (2014b) Seismic performance of ductile connections between precast beams and roof elements. Magazine of Concrete Research, 66(11):553-562, doi:10.1680/macr.13.00092

Belleri A, Torquati M, Riva P, Nascimbene R (2015) Vulnerability assessment and retrofit solutions of precast industrial structures. Earthquake and Structures, 8(3):801-820 doi:10.12989/eas.2015.8.3.801

Belleri A, Torquati M, Marini A, Riva P (2016) Horizontal cladding panels: in-plane seismic performance in precast concrete buildings. Bulletin of Earthquake Engineering, doi:10.1007/s10518-015-9861-8

Bellotti D, Bolognini D, Nascimbene R (2009) Response of traditional RC precast structures under cyclic loading. Environmental Semeiotics, 2(2):63-79

Biondini F, Dal Lago B, Toniolo G (2013) Role of wall panel connections on the seismic performance of precast structures. Bulletin of Earthquake Engineering, 11(4):1061-1081

Bournas DA, Negro P, Taucer FF (2014) Performance of industrial buildings during the Emilia earthquakes in Northern Italy and recommendations for their strengthening. Bulletin of Earthquake Engineering, 12(5):2383-2404

Brunesi E, Nascimbene R, Bolognini D, Bellotti D (2015) Experimental investigation of the cyclic response of reinforced precast concrete framed structures. PCI Journal, 15(2):57-79

Casotto C, Silva V, Crowley H, Nascimbene R, Pinho R (2015), Seismic Fragility of Italian RC Precast Industrial Structures. Engineering Structures, 94:122-136

CEN (2004), EN 1998-1:2004, Eurocode 8: Design of structures for earthquake resistance - Part 1: General rules, seismic actions and rules for buildings, European Committee for Standardization, Brussels, Belgium

Colombo A, Negro P, Toniolo G (2014) The influence of claddings on the seismic response of precast structures: the safecladding project. Proceedings of 2nd ECEES: 24-29 August 2014, Istanbul, Turkey

Colombo A, Negro P, Toniolo G, Lamperti M (2016) Design guidelines for precast structures with cladding panels, 2016, JRC Technical report, ISBN 978-92-79-58534-0

Dal Lago B, Toniolo G, Lamperti M (2016) Influence of different mechanical column-foundation connection devices on the seismic behaviour of precast structures. Bulletin of Earthquake Engineering, 14(12):3485–3508

Dal Lago B, Biondini F, Toniolo G, Lamperti M (2017) Experimental investigation on the influence of silicone sealant on the seismic behaviour of precast façades. Bulletin of Earthquake Engineering, 15(4):1771–1787

Dal Lago B, Biondini F, Toniolo G (2017) Experimental Investigation on Steel W-Shaped Folded Plate Dissipative Connectors for Horizontal Precast Concrete Cladding Panels, Journal Of Earthquake Engineering doi:10.1080/13632469.2016.1264333

Eligehausen R, Mallée R, Silva JF (2006) Anchorage in Concrete Construction, Ernst and Sohn, Berlin

Ferrara L, Felicetti R, Toniolo G, Zenti C (2011) Friction dissipative devices for cladding panels in precast buildings. European Journal of Environmental and Civil Engineering, 15(9):1319-1338

Fischinger M, Zoubek B, Isakovic T (2014) Seismic response of precast industrial buildings. Perspectives on European Earthquake Engineering and Seismology: Vol. 1. Ansal A (editor), Springer, Berlin, pp 131-177

Haber ZB, Saiidi MS, Sanders DH (2014) Seismic Performance of Precast Columns with Mechanically Spliced Column-Footing Connections. ACI Structural Journal, 111(3):639-650

Liberatore L, Sorrentino L, Liberatore D, Decanini LD (2013) Failure of industrial structures induced by the Emilia (Italy) 2012 earthquakes. Engineering Failure Analysis, 34:629-647

Magliulo G, Ercolino M, Petrone C, Coppola O, Manfredi G (2014a) The Emilia Earthquake: Seismic Performance of Precast Reinforced Concrete Buildings. Earthquake Spectra, 30(2):891-912

Magliulo G, Ercolino M, Cimmino M, Capozzi V, Manfredi G (2014b) FEM analysis of the strength of RC beam-to-column dowel connections under monotonic actions. Construction and Building Materials, 69:271–284

Magliulo G, Ercolino M, Manfredi G (2015) Influence of cladding panels on the first period of one-story precast buildings. Bulletin of Earthquake Engineering, 13(5):1531-1555

Marzo A, Marghella G, Indirli M (2012) The Emilia-Eomagna earthquake: damages to precast/prestressed reinforced concrete factories. Ingegneria Sismica, 29(2):132-147

641 Medina RA, Sankaranarayanan R, Kingston KM (2006) Floor response spectra for light components mounted on
642 regular moment-resisting frame structures. Engineering Structures, 28(14):1927-1940
643 Metelli G, Beschi C, Riva P (2011) Cyclic behaviour of a column to foundation joint for concrete precast structures.
644 European Journal of Environmental and Civil Engineering, 15(9):1297-1318
645 MidasGEN 2012 (v3.1), MIDAS Information Technologies Co. Ltd.
646 Minghini F, Ongaretto E, Ligabue V, Savoia M, Tullini N (2016) Observational failure analysis of precast buildings
647 after the 2012 Emilia earthquakes. Earthquake and Structures, 11(2):327-346
648 Nastri E, Vergato M, Latour M (2017) Performance evaluation of a seismic retrofitted R.C. precast industrial building
649 Earthquakes and Structures, Vol. 12, No. 1 (2017) 13-21
650 National Institute of Standards and Technology, NIST GCR 95-681 (1995) Literature Review on Seismic Performance
651 of Building Cladding Systems
652 Negro P, Bournas DA, Molina FJ (2013) Pseudodynamic tests on a full-scale 3-storey precast concrete building: Global
653 response. Engineering Structures, 57:594-608
654 Osanai Y, Watanabe F, Okamoto S (1996) Stress transfer mechanism of socket base connections with precast concrete
655 columns. ACI Structural Journal, 93(3):266-276
656 Takeda T, Sozen MA, Nielsen NN (1970): Reinforced concrete response to simulated earthquakes. Journal of the
657 Structural Division, 96(12):2557–2573
658 Palanci M, Senel SM, Kalkan A (2017) Assessment of one story existing precast industrial buildings in Turkey based
659 on fragility curves. Bulletin of Earthquake Engineering, 15(1):271-289
660 Pantoli E, Hutchinson TC, McMullin KM, Underwood GA, Hildebrand MJ (2016) Seismic-drift-compatible design of
661 architectural precast concrete cladding: tieback connections and corner joints. PCI journal, 61(4):38-52
662 Petrone C, Magliulo G, Manfredi G (2015) Seismic demand on light acceleration-sensitive nonstructural components in
663 European reinforced concrete buildings. Earthquake Engineering and Structural Dynamics, 44:1203–1217
664 Politopoulos I (2010) Floor Spectra of MDOF Nonlinear Structures, Journal of Earthquake Engineering, 14:5, 726-742
665 Psycharis IN, Mouzakis HP (2012) Shear resistance of pinned connections of precast members to monotonic and cyclic
666 loading. Engineering Structures, 41:413–427
667 Riva P, Franchi A, Tabeni D (2001) Welded Tempcore reinforcement behaviour for seismic applications, Materials and
668 Structures/Materiaux et Constructions, 34(238):240-247
669 Savoia M, Mazzotti C, Buratti N, Ferracuti B, Bovo M, Ligabue V, Vincenzi L (2012) Damages and collapses in
670 industrial precast buildings after the Emilia earthquake. Ingegneria Sismica, 29(2-3):120-131
671 Scotta R, De Stefani L, Vitaliani R (2015) Passive control of precast building response using cladding panels as
672 dissipative shear walls. Bulletin of Earthquake Engineering 13(11):3527-3552
673 Sullivan TJ, Calvi PM, Nascimbene R (2013) Towards improved floor spectra estimates for seismic design.
674 Earthquakes and Structures, 4(1): 109-132
675 Toniolo G, Colombo A (2012) Precast concrete structures: the lessons learned from the L'Aquila earthquake. Structural
676 Concrete, 13(2):73-83
677 Venmarcke EH, Gasparini DA (1976) Simulated Earthquake Motions Compatible with Prescribed Response Spectra –
678 SIMQKE-1. M.I.T. Department of Civil Engineering Research Report R76-4
679 Zoubek B, Fischinger M, Isakovic T (2015) Estimation of the cyclic capacity of beam-to-column dowel connections in
680 precast industrial buildings. Bulleting of Earthquake Engineering 13:2145–2168
681 Zoubek B, Fischinger M, Isaković T, (2016a) Cyclic response of hammer-head strap cladding-to-structure connections
682 used in RC precast building, Engineering Structures, 119:135-148
683 Zoubek B, Fischinger M, Isakovic T, (2016b) Seismic response of short restrainers used to protect cladding panels in
684 RC precast buildings. Journal of Vibration and Control, Doi 10.1177/1077546316659780